Analytical and Bioanalytical Chemistry (2018) 410:7979–7986
https://doi.org/10.1007/s00216-018-1420-0

RESEARCH PAPER

IR-MALDESI mass spectrometry imaging of underivatized neurotransmitters in brain tissue of rats exposed to tetrabromobisphenol A

M. Caleb Bagley[1] · Måns Ekelöf[1] · Kylie Rock[2,3] · Heather Patisaul[2,3] · David C. Muddiman[1,3,4]

Received: 6 August 2018 / Revised: 23 September 2018 / Accepted: 4 October 2018 / Published online: 13 October 2018

Abstract

There is a pressing need to develop tools for assessing possible neurotoxicity, particularly for chemicals where the mode of action is poorly understood. Tetrabromobisphenol A (TBBPA), a highly abundant brominated flame retardant, has lately been targeted for neurotoxicity analysis by concerned public health entities in the EU and USA because it is a suspected thyroid disruptor and neurotoxicant. In this study, infrared matrix-assisted laser desorption electrospray ionization (IR-MALDESI) coupled to a Q Exactive Plus mass spectrometer was used for the analysis of neurotransmitters in the brains of rats exposed to TBBPA in gestation and lactation through their mothers. Three neurotransmitters of interest were studied in three selected regions of the brain: caudate putamen, substantia nigra (SN), and dorsal raphe. Stable isotope labeled (SIL) standards were used as internal standards and a means to achieve relative quantification. This study serves as a demonstration of a new application of IR-MALDESI, namely that neurotransmitter distributions can be confidently and rapidly imaged without derivatization.

Keywords IR-MALDESI · Neurotransmitters · Mass spectrometry imaging · Exposomics · Orbitrap

Introduction

The distribution of neurotransmitter (NT) abundance differs markedly across brain nuclei and subregions, and disruption of NT levels can be an important indicator of neurotoxicity and/or disease. Notorious examples are organophosphate and carbamate pesticides that, like their nerve agent chemical cousins, inhibit acetylcholine breakdown and can result in severe neural damage and even death. NT distribution and/or function can also be sexually dimorphic, yielding insight as to why some diseases have sex-biased incidences. A well-characterized example is the maturation of gamma-aminobutyric acid (GABA), where receptor-mediated signaling patterns which are age- and sex-specific can help coordinate sexually dimorphic brain development [1]. For many suspected neurotoxicants and/or disease states, however, NT-related impacts are unknown and difficult to measure across large regions. Thus, the capacity to detect subtle and region-specific changes in NTs, including their sexually dimorphic distribution, would represent a significant technical advancement that would help link environmental exposures with neural disease.

Upwards of 90,000 synthetic chemicals have been developed for industrial and commercial use over the past century, although a full accounting has proved virtually impossible, even for regulators such as the US Environmental Protection Agency [2]. Very few of these chemicals have been specifically tested for neurotoxicity, but of those, epidemiological studies have associated 200+ chemicals with neurotoxicity

Electronic supplementary material The online version of this article (https://doi.org/10.1007/s00216-018-1420-0) contains supplementary material, which is available to authorized users.

✉ David C. Muddiman
david_muddiman@ncsu.edu

[1] FTMS Laboratory for Human Health Research, Department of Chemistry, North Carolina State University, Raleigh, NC 27695, USA

[2] Department of Biological Sciences, North Carolina State University, Raleigh, NC 27695, USA

[3] Center for Human Health and the Environment, North Carolina State University, Raleigh, NC 27691, USA

[4] Molecular Education, Technology and Research Innovation Center (METRIC), North Carolina State University, Raleigh, NC 27695, USA

in humans [3]. Common to many neural disorders is the disruption of neurotransmitters and neurotransmission, making this a particularly critical area for toxicity testing and methods development. Here, we describe a novel approach for analyzing neurotransmitter disruption in rodent brain slices and demonstrate how this might be used in future studies assessing neurotoxicity.

Chemical FRs have been identified as particularly concerning because exposure is nearly unavoidable, with levels higher in children than adults [4, 5]. Many bioaccumulate, are long lived, and linked with neurodevelopmental and other adverse outcomes in humans [6]. FRs were effectively mandated into the US consumer products market when California implemented Technical Bulletin 117 in 1975, requiring that furniture upholstery fabric and filling materials pass certain flammability tests prior to production [7]. Currently, one of the most abundant FRs by production volume is tetrabromobisphenol A (TBBPA) [8]. Human exposure to TBBPA usually occurs through dermal contact, inhalation, and/or ingestion. Several brominated FRs have been shown to persist in human milk and adipose tissue [9], including TBBPA [10]. Recent analyses have shown that it can act as a hormone manipulator in the thyroid [11] and has the potential to be carcinogenic [12] and neurotoxic [13]. Its primary mode of action remains unknown, but of high interest, which is why it was selected for this proof of concept study.

Mass spectrometry imaging (MSI) can be leveraged to provide comprehensive data on NTs of interest, and with further data analysis, can reveal new information regarding associated biochemical pathways and products. MSI offers an excellent way of visualizing different types of biomolecular ions, including NTs, in discrete spatial locations [14]. The fundamentals of ion generation necessary for many current MSI approaches were introduced in two seminal techniques. One of those, matrix-assisted laser desorption/ionization (MALDI) [15, 16], uses a laser beam to ablate sample material and generate molecular ions and the other, electrospray ionization (ESI) [17], employs a charged droplet spray to analyze the sample. Both techniques have enhanced the field of MSI by enabling the ionization of large, intact biomolecules. From these, two grandfather techniques have come many others. In fact, NTs and biomolecular ions of interest have been imaged with MSI using techniques such as MALDI [18, 19], LAESI [20], nano-DESI and DESI [21, 22], and TOF-SIMS [23]. Herein, we present the use of IR-MALDESI [24, 25], a hybridization of MALDI and ESI, which affords a new rapid, matrix-free and derivatization-free analysis of NTs [26].

Analysis of derivatization-free NTs is an important benefit of MALDESI because derivatization has some inherent disadvantages. Chief among them are increased costs and the time-consuming workflow that hamper rapid hypothesis testing. Additionally, it can result in byproduct formation and losing sensitivity to other important analytes. Our work demonstrates that we do not need derivatization to accomplish many of the benefits it offers. For example, we have no need to increase selectivity, one of the main reasons for using derivatization, as the NTs of interest can be adequately isolated and measured [27, 28]. Based on the strengths of our methodology derivatization disadvantages are not worth its potential benefits. Although derivatization-free NTs have been analyzed with (nano-) DESI [21, 22], MALDESI offers greater ability for absolute quantitation since all tissue is ablated and as such, this paper presents the foundation for future MALDESI derivatization-free NT work.

Since its inception, IR-MALDESI has evolved into a rapid, ambient MSI technique and expanded its analyte characterization range to enable effective and detailed characterization of NT and low *m/z*-molecular ion abundances in complex biochemical environments. The results of this project constitute an analytical step forward for IR-MALDESI and demonstrate its viability as a technique for adding important spatial and abundance information of NTs relevant to behavior, neurotoxicity, and neural disease.

Experimental

Materials

High-purity liquid chromatography (HPLC) grade water was purchased from Fisher Scientific (Fair Lawn, NJ, USA), and HPLC grade methanol was purchased from Burdick & Jackson (Muskegon, MI, USA). A 0.2% formic acid (Fluka Analytical, Morris Plains, NJ) solution was made in 50:50 methanol:water as the electrospray solvent. ^{13}C labeled standards of 4-aminobutyric acid (GABA; $13C_4$-GABA) and dopamine (DA; Ring-$^{13}C_6$-DA) were acquired from Cambridge Isotope Laboratories, Inc. (Tewksbury, MA, USA). Nitrogen gas used to purge the sample stage enclosure of humidity was purchased from Arc3 Gases (Raleigh, NC, USA).

Biological samples preparation

Time pregnant Harlan Sprague Dawley rats (Envigo) were shipped to the National Institute of Environmental Health Sciences (NIEHS) on gestational day (GD) 4 or 5. Day of visual confirmation of sperm plugs was considered as GD 0. Upon arrival, dams were weighed and randomly assigned to 5 dose groups based on body weight (BW) ($n = 8$–9 per dose groups) with equal representation from each gestational block. For the present study, only two dose groups were used: Dams were orally exposed to 0 or 10 mg TBBPA/kg BW twice a day at 7 am and 1 pm, GD 6 through postnatal day (PND) 21. Tetrabromobisphenol A (TBBPA) (Sigma-Aldrich, Cas # 79-94-7, assay 97%, lot #MKBG4059V) was prepared in

refined sesame seed oil (Jedwards International, Inc., Braintree, MA) for the targeted concentrations (0 and 10 mg TBBPA/kg BW) to be administered to rats in the volume of 5 ml/kg bw. The concentrated solutions were color coded for blinded allocation. Litters were equalized to 8 on PND 4 and pups were fostered into small litters from the same dose group. Dams were singly housed in polysulfone caging with Sani-Chip Bedding (PJ Murphy Products, Montville, NJ) with Enviro-Dri enrichment (Shepherd Speciality Papers, Watertown, TN) and maintained on Teklad 2919 low phytoestrogen (Envigo Laboratories, Madison, WI). Animals were held in humidity-and-temperature controlled room with 12-h light cycles (lights on at 7 am) at 25 °C and 45–60% average humidity. Food and water were given ad libitum. On PND 21, pups were weaned and caged 2–3 per sex per litter to ensure socialization. Pups were aged out (approx. PND 115) and transported to the Biological Resources Facility at NCSU (20 min drive away) for locomotor behavioral testing (data to be reported elsewhere) and brain analysis. Housing conditions including diet, caging, bedding, and light cycles were as identical as possible to the NIEHS facility.

After behavioral analysis, animals were sacrificed by CO_2 asphyxiation and rapid decapitation. Brains were removed, flash frozen on powdered dry ice, wrapped in foil, and stored in a Forma ULT − 80 °C freezer (Thermo, Waltham, MA, USA) until they were coronally sectioned on a CM1950 cryostat (Leica, Buffalo Grove, IL, USA) at − 20 °C into 20-μm-thick sections at the time of analysis. These sections were thaw mounted on the slides pre-conditioned with SIL-GABA (4.7 mM) and SIL-DA (6.3 mM) and placed in the MALDESI source [29]. Sample-to-sample technical variability was minimized by applying SIL standards to the sample slides at the aforementioned concentrations, to give a consistent denominator by which to compare signals from the analyte of interest. As the laser ablates tissue, it also ablates the standards underneath. Since they are SIL molecules of our NTs of interest, they have similar ionization efficiencies and ablation dynamics across each tissue. This diminishes much of the difficulty of comparing across different sampling conditions and variability. Therefore, the ratio elucidates the true biology of the sample.

All animal work was done according to the applicable portions of the Animal Welfare Act and the U.S. Department of Health and Human Services Guide for the Care and use of Laboratory Animals. All aspects of the rat studies were approved by the Institutional Animal Care and Use Committees of NIEHS and NCSU.

Midlevel coronal sections containing three regions of interest were selected for this study because of their known NT abundance: caudate putamen (− 0.12 mm from Bregma; DA rich), substantia nigra (− 4.92 from Bregma; DA and GABA rich), and dorsal raphe (− 7.8 from Bregma; 5-HT rich). Sections were identified with the assistance of a brain atlas [30] as we have done previously [31, 32] using well-characterized landmarks including the location and size of the anterior commissure, corpus callosum and lateral ventricles for the caudate putamen, hippocampal layers, dorsal third ventricle and medial mammillary nucleus for the substantia nigra, and aqueduct, pontine nuclei, and remnants of the pineal gland for the dorsal raphe. Adjacent sections were slide mounted and NISSL stained to confirm anatomical precision.

IR-MALDESI imaging source

The imaging source and experimental procedures have been described in its recent configuration previously [24]. A mid-IR (2.94 μm) laser from JGMA Associates (Burlington, MA, USA) was used for laser sampling in all experiments [33]. Tissue regions of interest were imaged at 200-μm spatial resolution, with each mass spectrum generated from a single burst of 10 pulses of 100 μJ at 10 kHz. A Q Exactive Plus mass spectrometer (Thermo Fisher Scientific, Bremen, Germany) was used for all experiments, with an ion injection time (IT) of 25 ms. All spectra were collected in positive ion mode from 100 to 400 *m/z*, at a nominal resolving power of $140{,}000_{FWHM}$ at *m/z* 200. The main difference in experimental procedures involved working at an ESI flow rate of 1 μL/min as opposed to 2 μL/min.

Ice matrix application

The protocols for biological tissue imaging have been described in detail in previous publications [24]. Prior to analysis, each sample was placed on a Peltier-cooled sampling stage inside a sealed enclosure, purged with nitrogen gas to < 10% relative humidity, and cooled down to − 8 °C. The enclosure was then opened up to ambient air with 30–35% relative humidity to form an ice layer over the sample over the course of 10 min. During all experiments, the enclosure was kept open throughout analysis as the ice layer did not have time to build up too much.

Data analysis

Image analysis was performed using the open source imaging interface MSiReader [34, 35]. XCalibur raw files (Thermo Fisher, Scientific, Bremen, Germany) were converted to imzML file using the MSConvert application [36] to convert raw files to mzML files and then converting the mzML files to imzML files using ImzMLconvert [36, 37]. MSiReader was used to generate ion abundance distribution images. Untargeted searching was performed using the MSiPeakfinder tool [35] to identify ion distributions of interest. The molecular ions of targeted neurotransmitter were imaged normalized to their corresponding SIL compound, which

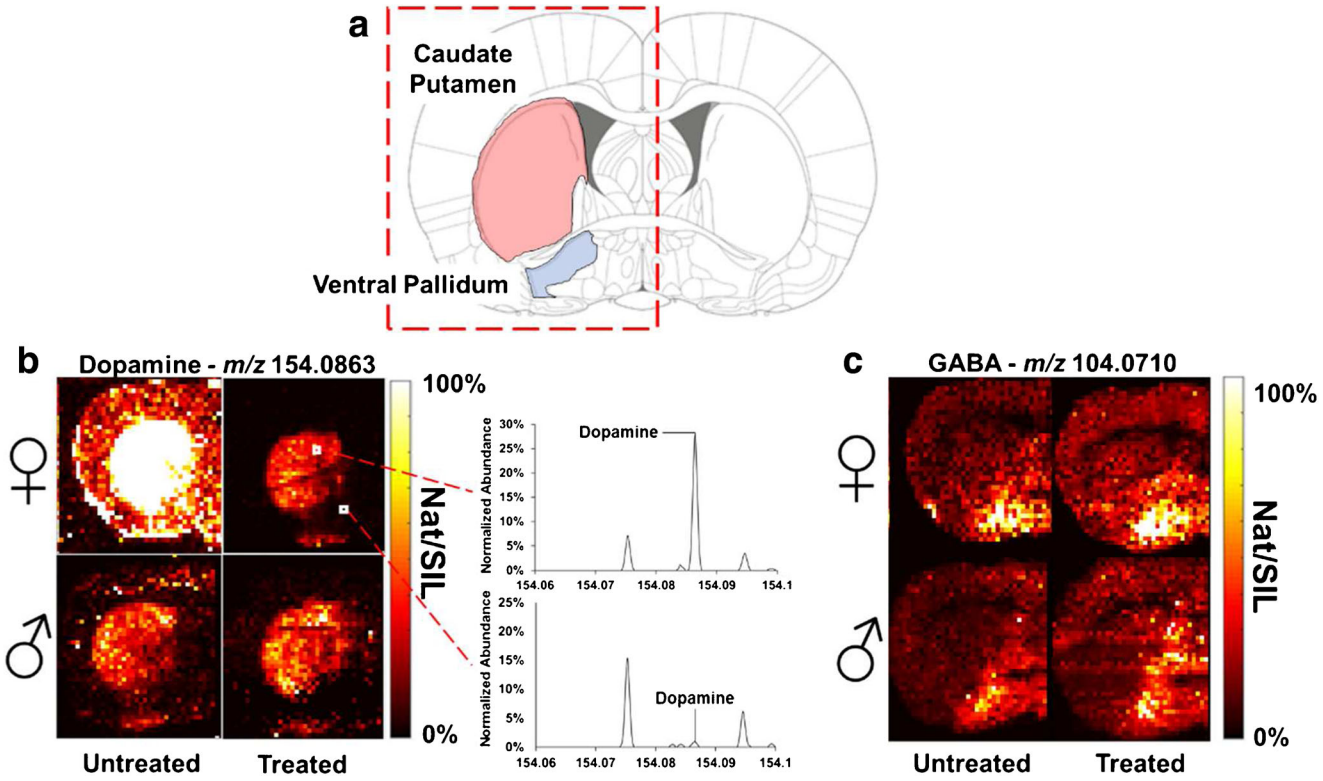

Fig. 1 Ion abundance heat maps in the caudate putamen (**a**) for dopamine (*m/z* 154.0863, **b**) and GABA (*m/z* 104.0710, **c**) normalized to their SIL isotopes. The inset abundance charts demonstrate an example of the difference between bright and dark voxels in the images. The top row of each image set are female samples, the bottom row are males. The left columns are untreated rats, the right columns are treated rats. The red dashed box shows the region of the brain sample that was analyzed

greatly aided in the formation of images representative of the inherent biology of the samples.

Results and discussion

Targeted neurotransmitter study

This study analyzed vital regions for three key NTs, selected for their biological relevance. The most rostral region selected was a section containing the caudate putamen (see Electronic Supplementary Material (ESM) Image S3). Part of the striatum, this region is richly innervated by glutamatergic and dopaminergic inputs from different sources including the other basal ganglia. This section also included the ventral pallidum, a striatal region heavily populated with GABAergic neurons, and the bed nucleus of the stria terminalis (BnST) which is sexually dimorphic in many regards including the density of GABA neurons [1, 38]. This brain section was analyzed specifically for DA and GABA in an effort to determine if DA and GABA distributions mirrored known regional and sex-specific patterns. As expected, levels of DA and GABA were highest in the regions of interest (a representative example can be found in ESM Figs. S4, S5,

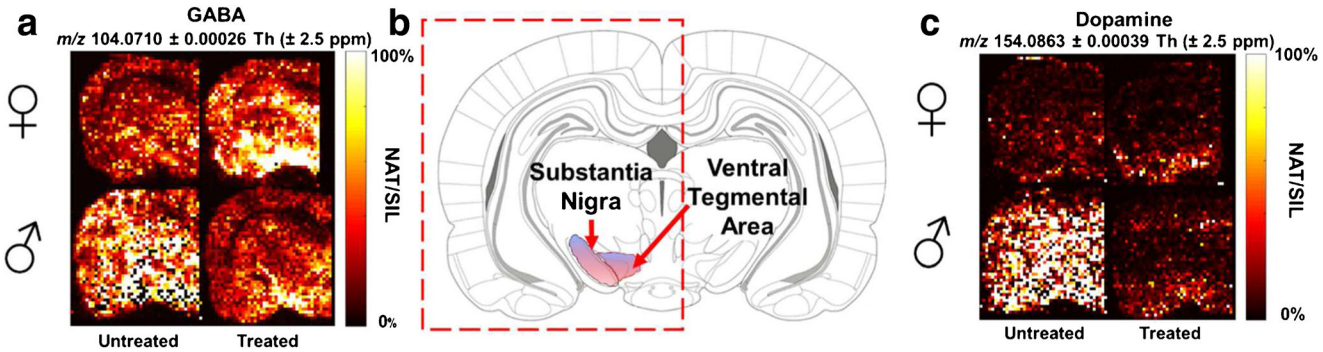

Fig. 2 Image of GABA (*m/z* 104.0710, **a**) and dopamine (*m/z* 154.0863, **c**) distributions normalized to SIL-GABA and SIL-DA, respectively, in the Substantia nigra and ventral tegmental area (**b**)

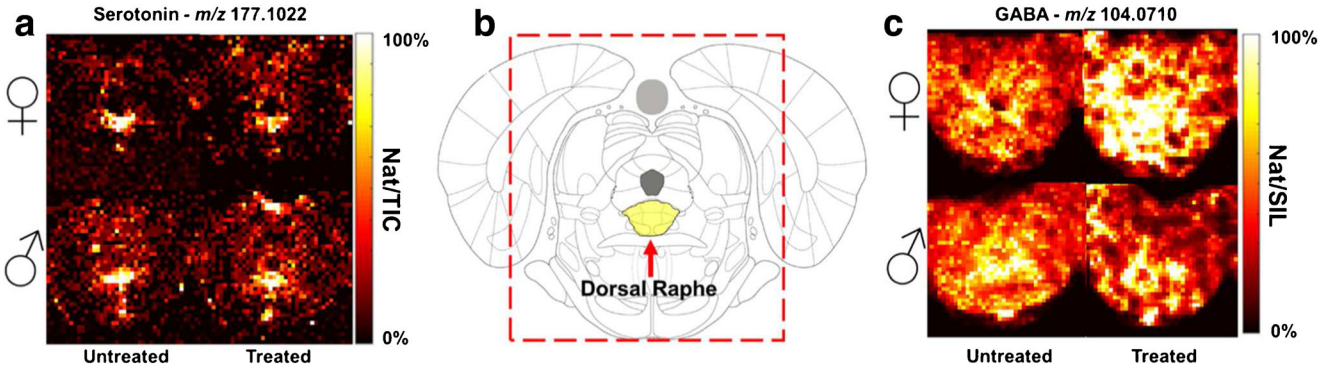

Fig. 3 Image **a** demonstrates the bundle of serotonergic neurons in the Dorsal raphe (**b**) by imaging serotonin (*m/z* 177.1022). GABA (*m/z* 104.0710, **c**) was also imaged. Note: Natural serotonin abundances are normalized to TIC (total ion current) while GABA is normalized to SIL-GABA

S6), with DA defining the borders of the caudate putamen and ventral pallidum, and only trace levels detected in the cortex and other surrounding structures of either sex (Fig. 1). Some differences in DA abundances in the few samples analyzed were observed, particularly in the surrounding cortical regions, which compels further investigation.

Substantia Nigra (SN) and the neighboring ventral tegmental area (VTA) were also analyzed (ESM Image S1) because both are enriched with DA and GABA. GABA was readily detectable in the SN and VTA, although the two could not be distinguished from each other. Trace levels of GABA were also visible in the amygdala of both sexes (Fig. 2). Although this sample size is small, the differences between sexes and treatments garner a larger future study to quantify possible differences. Although preliminary, and inconclusive, these possible effects are particularly intriguing because the SN and VTA have already been identified as possibly vulnerable to TBBPA. Here, we have demonstrated how MALDESI can provide the high-quality imaging that would be invaluable to such a study.

The dorsal raphe was the most caudal region selected (ESM Image S3) and is by far the largest serotonergic nucleus in the brain, providing a substantial proportion of forebrain serotonin (5-HT) innervation. Densely populated with 5-HT neurons in both sexes, this brain stem region is thought to be the primary target of selective

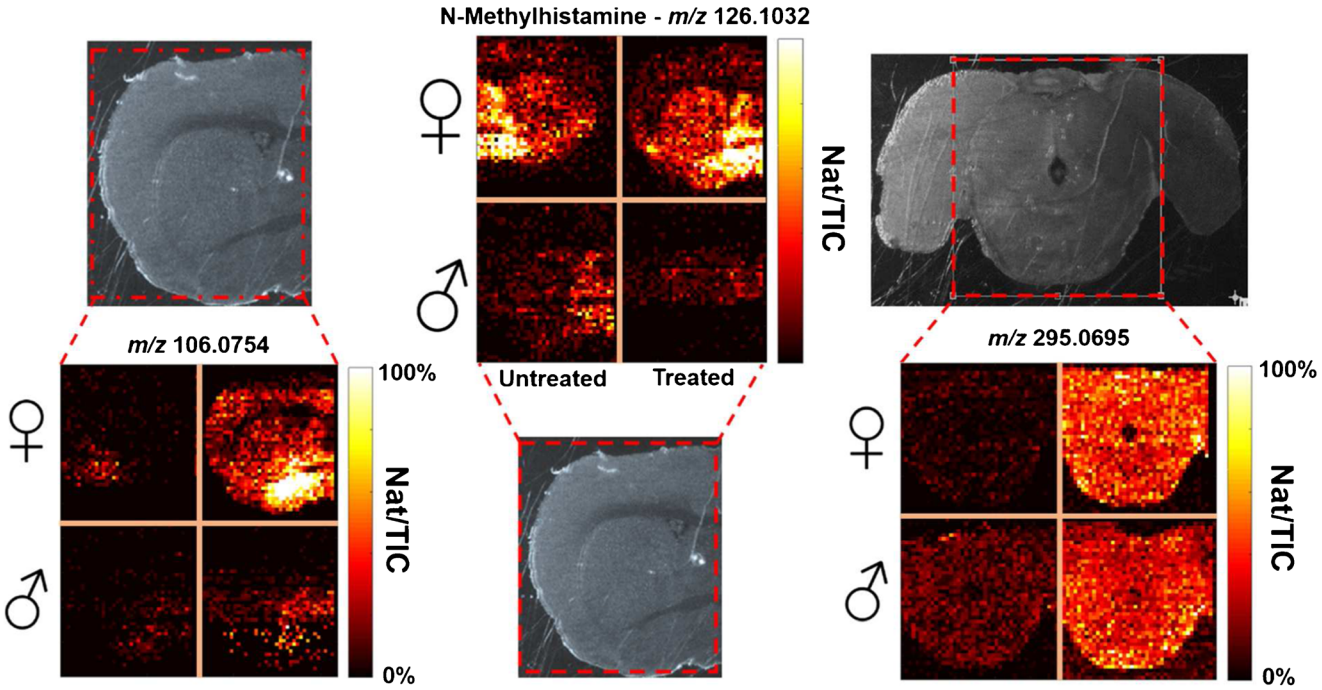

Fig. 4 Three images of molecular ions identified through an untargeted search of the whole dataset. The middle image is estimated by atomic composition to be *N*-methylhistamine (*m/z* 126.1032). The image on the left is ion at *m/z* 106.0754 with highest abundances in the treated female. The image on the right is of *m/z* 295.0695 which occurs with higher abundance in treated samples of both male and female. Each image is connected to the image of the sampled region for identification. Abundances are reported as relative to TIC

serotonin reuptake inhibitors and is associated with behaviors related to mood and motivation. GABA is present throughout this nucleus and the surrounding structures but not confined to specific substructures. The neurotransmitter distributions in Fig. 3 show a wide, diffuse distribution of GABA and the tight, concentrated area of 5-HT [39]. As expected, the pattern of 5-HT (Fig. 3) was largely confined to the raphe nuclei, with the greatest concentration detected in the dorsal raphe, located just below the cerebral aqueduct. By contrast, GABA was more diffuse, likely reflecting the presence of extrasynaptic GABA(A) receptors throughout the region. Density was generally highest in the medioventral portion of the brain stem. Further studies with additional biological replicates will be required to establish if levels differ by sex or TBBPA exposure, but these results confirm that MALDESI is capable of detecting region-specific levels of 5-HT.

N-Methylhistamine and neurotransmitter sexual dimorphism

Image analysis led to findings that corroborate biological understanding, and raise interesting questions. Although not initially targeted for analysis, *N*-methylhistamine was found to colocalize strongly with GABA in the caudate putamen for the female samples (Fig. 4). This observation contributes high-quality visual corroboration to previous reports stating that histamine and GABA are co-transmitted to regulate awakeness [40]. Documentation of a sex difference is consistent with what numerous other studies have determined previously; histamine metabolism is much higher in females than males [41, 42]. Both treated and untreated female samples have greater abundance of this histamine metabolite (*N*-methylhistamine) than either of the male samples (Fig. 4).

N-Methylhistamine is just one initially untargeted NT that was found to be sexually dimorphic and/or TBBPA sensitive. An undetermined ion at 106.0754 *m/z* showed very high abundances in the caudate putamen for the treated female only. Another undetermined *m/z* 295.0695 showed up in the brain stem images in far greater abundance in both treated samples than either of the untreated (Fig. 4). In each case, neither *m/z* has a readily identifiable chemical formula but is of obviously high interest for understanding how TBBPA may impact brain function and could represent a novel mode of action in each sex. Future studies will carry out MS/MS for all interesting distributions, including those presented here and found in ESM (Figs. S1, S2, S3 and Table S1). Collectively, the findings presented herein demonstrate the utility of MALDESI for identifying substructures and low *m/z* NTs of interest in brain tissue.

Conclusions

The results from this study demonstrate that IR-MALDESI is a suitable method for imaging neurotransmitters in brain tissue and is sensitive enough to detect intrinsic sex differences. Using the developed experimental protocol, fresh brain tissue can be analyzed for underivatized, matrix-free neurotransmitters using SIL coated slides for relative quantification by normalization. As such, this constitutes a strong foundation for larger projects that need consistent analysis of multiple replicates in a reasonable time frame (The method as presented requires less than 20 min per hemisphere section). Neurobiologists can employ IR-MALDESI as a practical and powerful analytical tool for testing hypotheses regarding the chemical composition of a brain and how that composition might be disrupted by environmental factors such as chemical exposures.

Acknowledgements All mass spectrometry measurements were made in the Molecular Education, Technology, and Research Innovation Center (METRIC) at NC State University. We are grateful for the NIEHS research team who designed and executed the TBBPA exposure portion of this project, especially Suzanne Fenton, Manushree Bharadwaj, Joshua Warmack, and Sagi Enicole Gillera.

Funding information This study received financial assistance from the National Institutes of Health grants R01GM087964 (MCB, ME, DM) and P30ES025128 to North Carolina State University as well as a National Institutes of Health IPA Agreement with HP.

Compliance with ethical standards

All aspects of the rat studies were approved by the Institutional Animal Care and Use Committees of NIEHS and NCSU.

Conflict of interest The authors declare that they have no conflicts of interest

References

1. Galanopoulou AS. Sexually dimorphic expression of KCC2 and GABA function. Epilepsy Res. 2008. https://doi.org/10.1016/j.eplepsyres.2008.04.013.
2. How many chemicals are in use today? C&EN Global Enterp. 2017. https://doi.org/10.1021/cen-09509-govpol.
3. Heyer DB, Meredith RM. Environmental toxicology: sensitive periods of development and neurodevelopmental disorders. Neurotoxicology. 2017.
4. Malliari E, Kalantzi O. Children's exposure to brominated flame retardants in indoor environments - a review. Environ Int. 2017;108:146–69.
5. Sugeng EJ, de Cock M, Schoonmade LJ, van de Bor M. Toddler exposure to flame retardant chemicals: magnitude, health concern and potential risk- or protective factors of exposure: observational studies summarized in a systematic review. Chemosphere. 2017;184:820–31.
6. Dingemans MML, van dB, Westerink RHS. Neurotoxicity of brominated flame retardants: (in)direct effects of parent and hydroxylated polybrominated diphenyl ethers on the (developing) nervous

system. Environ Health Perspect. 2011. https://doi.org/10.1289/ehp.1003035.
7. Stapleton HM, Sharma S, Getzinger G, Ferguson PL, Gabriel M, Webster TF, et al. Novel and high volume use flame retardants in US couches reflective of the 2005 PentaBDE phase out. Environ Sci Technol. 2012. https://doi.org/10.1021/es303471d.
8. Knudsen GA, Hughes MF, McIntosh KL, Sanders JM, Birnbaum LS. Estimation of tetrabromobisphenol A (TBBPA) percutaneous uptake in humans using the parallelogram method. Toxicol Appl Pharmacol. 2015. https://doi.org/10.1016/j.taap.2015.09.012.
9. Antignac JP, Cariou R, Zalko D, Berrebi A, Cravedi JP, Maume D, et al. Exposure assessment of French women and their newborn to brominated flame retardants: determination of tri- to deca-polybromodiphenylethers (PBDE) in maternal adipose tissue, serum, breast milk and cord serum. Environ Pollut. 2009. https://doi.org/10.1016/j.envpol.2008.07.008.
10. Cariou R, Antignac JP, Zalko D, Berrebi A, Cravedi JP, Maume D, et al. Exposure assessment of French women and their newborns to tetrabromobisphenol-A: occurrence measurements in maternal adipose tissue, serum, breast milk and cord serum. Chemosphere. 2008. https://doi.org/10.1016/j.chemosphere.2008.07.084.
11. Lai DY, Kacew S, Dekant W. Tetrabromobisphenol A (TBBPA): possible modes of action of toxicity and carcinogenicity in rodents. Food Chem Toxicol. 2015. https://doi.org/10.1016/j.fct.2015.03.023.
12. National TP. NTP technical report on the toxicology studies of tetrabromobisphenol A (CASRN 79-94-7) in F344/NTac rats and B6C3F1/N mice and toxicology and carcinogenesis studies of tetrabromobisphenol A in Wistar Han Crl:WI(Han)] rats and B6C3F1/N mice (gavage studies). U.S. Department of Health and Human Services, Public Health Service, National Institutes of Health, National Toxicology Program. 2014.
13. Nakajima A, Saigusa D, Tetsu N, Yamakuni T, Tomioka Y, Hishinuma T. Neurobehavioral effects of tetrabromobisphenol A, a brominated flame retardant, in mice. Toxicol Lett. 2009. https://doi.org/10.1016/j.toxlet.2009.05.003.
14. Chughtai K, Heeren RMA. Mass spectrometric imaging for biomedical tissue analysis. Chem Rev. 2010. https://doi.org/10.1021/cr100012c.
15. Tanaka K, Waki H, Ido Y, Akita S, Yoshida Y, Yoshida T, et al. Protein and polymer analyses up to m/z 100 000 by laser ionization time-of-flight mass spectrometry. Rapid Commun Mass Spectrom. 1988. https://doi.org/10.1002/rcm.1290020802.
16. Karas M, Hillenkamp F. Laser desorption ionization of proteins with molecular masses exceeding 10,000 daltons. Anal Chem. 1988. https://doi.org/10.1021/ac00171a028.
17. Fenn JB, Mann M, Meng CK, Wong SF, Whitehouse CM. Electrospray ionization for mass spectrometry of large biomolecules. Science. 1989. https://doi.org/10.1126/science.2675315.
18. Norris JL, Caprioli RM. Analysis of tissue specimens by matrix-assisted laser desorption/ionization imaging mass spectrometry in biological and clinical research. Chem Rev. 2013. https://doi.org/10.1021/cr3004295.
19. Shariatgorji M, Nilsson A, Goodwin RJ, Kallback P, Schintu N, Zhang X, et al. Direct targeted quantitative molecular imaging of neurotransmitters in brain tissue sections. Neuron. 2014. https://doi.org/10.1016/j.neuron.2014.10.011.
20. Nemes P, Woods AS, Vertes A. Simultaneous imaging of small metabolites and lipids in rat brain tissues at atmospheric pressure by laser ablation electrospray ionization mass spectrometry. Anal Chem. 2010. https://doi.org/10.1021/ac902245p.
21. Bergman HM, Lundin E, Andersson M, Lanekoff I. Quantitative mass spectrometry imaging of small-molecule neurotransmitters in rat brain tissue sections using nanospray desorption electrospray ionization. Analyst. 2016. https://doi.org/10.1039/c5an02620b.
22. Fernandes AMAP, Vendramini PH, Galaverna R, Schwab NV, Alberici LC, Augusti R, et al. Direct visualization of neurotransmitters in rat brain slices by desorption electrospray ionization mass spectrometry imaging (DESI - MS). J Am Soc Mass Spectrom. 2016. https://doi.org/10.1007/s13361-016-1475-0.
23. Passarelli MK, Winograd N. Lipid imaging with time-of-flight secondary ion mass spectrometry (ToF-SIMS). Biochim Biophys Acta. 2011. https://doi.org/10.1016/j.bbalip.2011.05.007.
24. Bokhart MT, Muddiman DC. Infrared matrix-assisted laser desorption electrospray ionization mass spectrometry imaging analysis of biospecimens. Analyst. 2016. https://doi.org/10.1039/c6an01189f.
25. Robichaud G, Barry J, Muddiman D. IR-MALDESI mass spectrometry imaging of biological tissue sections using ice as a matrix. J Am Soc Mass Spectrom. 2014. https://doi.org/10.1007/s13361-013-0787-6.
26. Esteve C, Tolner EA, Shyti R, van dM, McDonnell LA. Mass spectrometry imaging of amino neurotransmitters: a comparison of derivatization methods and application in mouse brain tissue. Metabolomics. 2016. https://doi.org/10.1007/s11306-015-0926-0.
27. Sakino T, Yuki S, Akiko K, Mitsuyo O, Sachise K, Toshimi M, et al. Microscopic imaging mass spectrometry assisted by on-tissue chemical derivatization for visualizing multiple amino acids in human colon cancer xenografts. Proteomics. 2014. https://doi.org/10.1002/pmic.201300041.
28. Shariatgorji M, Nilsson A, Goodwin RA, Källback P, Schintu N, Zhang X, et al. Direct targeted quantitative molecular imaging of neurotransmitters in brain tissue sections. Neuron. 2014;84:697–707.
29. Bokhart MT, Rosen E, Thompson C, Sykes C, Kashuba ADM, Muddiman DC. Quantitative mass spectrometry imaging of emtricitabine in cervical tissue model using infrared matrix-assisted laser desorption electrospray ionization. Anal Bioanal Chem. 2015. https://doi.org/10.1007/s00216-014-8220-y.
30. Paxinos G, Watson C. The rat brain in stereotaxic coordinates. London: Academic Press; 2007.
31. Arambula SE, Fuchs J, Cao J, Patisaul HB. Effects of perinatal bisphenol A exposure on the volume of sexually-dimorphic nuclei of juvenile rats: a CLARITY-BPA consortium study. NeuroToxicology. 2017;63:33–42.
32. Cao J, Joyner L, Mickens JA, Leyrer SM, Patisaul HB. Sex-specific Esr2 mRNA expression in the rat hypothalamus and amygdala is altered by neonatal bisphenol A exposure. Reproduction. 2014. https://doi.org/10.1530/rep-13-0501.
33. Ekelöf M, Manni J, Nazari M, Bokhart M, Muddiman DC. Characterization of a novel miniaturized burst-mode infrared laser system for IR-MALDESI mass spectrometry imaging. Anal Bioanal Chem. 2018. https://doi.org/10.1007/s00216-018-0918-9.
34. Robichaud G, Garrard KP, Barry JA, Muddiman DC. MSiReader: an open-source interface to view and analyze high resolving power MS imaging files on Matlab platform. J Am Soc Mass Spectrom. 2013. https://doi.org/10.1007/s13361-013-0607-z.
35. Bokhart MT, Nazari M, Garrard KP, Muddiman DC. MSiReader v1.0: evolving open-source mass spectrometry imaging software for targeted and untargeted analyses. J Am Soc Mass Spectrom. 2017. https://doi.org/10.1007/s13361-017-1809-6.
36. Chambers MC, Maclean B, Burke R, Amodei D, Ruderman DL, Neumann S, et al. A cross-platform toolkit for mass spectrometry and proteomics. Nat Biotechnol. 2012. https://doi.org/10.1038/nbt.2377.

37. Race AM, Styles IB, Bunch J. Inclusive sharing of mass spectrometry imaging data requires a converter for all. J Proteomics. 2012. https://doi.org/10.1016/j.jprot.2012.05.035.
38. Hines M, Allen LS, Gorski RA. Sex differences in subregions of the medial nucleus of the amygdala and the bed nucleus of the stria terminalis of the rat. Brain Res. 1992;579:321–6.
39. Frazer A, Hensler JG. Anonymous basic neurochemistry molecular, cellular and medical aspects. 6th ed. Philadelphia: Lippincott-Raven; 1999.
40. Yu X, Ye Z, Houston C, Zecharia A, Ma Y, Zhang Z, et al. Wakefulness is governed by GABA and histamine cotransmission. Neuron. 2015. https://doi.org/10.1016/j.neuron.2015.06.003.
41. Ponvert C, Galoppin L, Scheinmann P, Canu P, Burtin C. Tissue histamine levels in male and female mast cell deficient mice (W/Wv) and in their littermates (Wv/+, W/+ and +/+). Agents Actions. 1985. https://doi.org/10.1007/BF01966671.
42. Netter KJ, Cohn VH, Shore PA. Sex difference in histamine metabolism in the rat. Am J Physiol. 1961. https://doi.org/10.1152/ajplegacy.1961.201.2.224.